Approximate Noise Temperature Calculations of Offset Gregorian Reflector Systems

Robert Lehmensiek[1], and Dirk I.L. de Villiers[2]
[1]Department of Electrical Engineering, Cape Peninsula University of Technology, Bellville 7530, South Africa
[2] 1Department of Electrical and Electronic Engineering, Stellenbosch University, Stellenbosch, 7600, South Africa

***Abstract* - Accurate antenna noise temperature calculations of an offset Gregorian reflector system over a wide frequency band is computationally expensive. The main reflector masking technique, which removes the main reflector from the calculation domain, considerably reduces the computational cost, but for an electrically small reflector system, diffraction effects affect the accuracy. Recently improvements to this technique were proposed by introducing correction factors. In this paper we investigate the improvement in accuracy using higher order compensation factors, frequency subdivision, and direct interpolation of the residual of the antenna temperatures.**

***Index Terms* — Noise temperature, radio astronomy, receiving sensitivity, reflector antennas.**

1. Introduction and Interpolation Techniques

An important metric (which needs to be accurately predicted) for radio telescopes is receiving sensitivity. This is the ratio of effective aperture area to system noise temperature (A_e/T_{sys}), where the system noise temperature is the sum of receiver (assumed here to be 10 K) and antenna noise temperatures. Calculating antenna noise temperature,

$$T_A(f\,|\,\theta_p)=\frac{\iint_{4\pi}T_b(f,\theta,\phi)P(f,\theta,\phi)\sin\theta\,d\theta\,d\phi}{\iint_{4\pi}P(f,\theta,\phi)\sin\theta\,d\theta\,d\phi}, \quad (1)$$

entails integrating the product of the antenna radiation pattern P with the surrounding scene brightness temperature T_b [1] (defined in the standard spherical coordinate system with azimuthal and polar angles ϕ and θ) over the entire 4π steradian sphere, and this is determined over both antenna elevation angles θ_p and frequency f. Calculating (1) is often a computationally expensive task for reflector systems, due to a prohibitively large number of radiation pattern samples required to ensure convergence of the noise temperature integral, and the calculation of the antenna noise temperature itself. The main reflector masking technique, which was proposed in [2], approximates the antenna noise temperature calculation, as follows:

$$T_A(f\,|\,\theta_p)\approx T_A^{mask}(f\,|\,\theta_p)=\frac{\iint_{4\pi}T_b^{mask}(f,\theta,\phi)P^{no\_MR}(f,\theta,\phi)\sin\theta\,d\theta\,d\phi}{\iint_{4\pi}P^{no\_MR}(f,\theta,\phi)\sin\theta\,d\theta\,d\phi}, \quad (2)$$

where P^{no_MR} is the total antenna radiation pattern with the main reflector removed from the electromagnetic calculation domain, and T_b^{mask} is the brightness temperature that includes a masked region with temperature T^{α}. The masked region is the angular extent of the scattered energy from the sub-reflector (in transmit mode) in the direction of the main reflector. This is illustrated in Fig. 1.

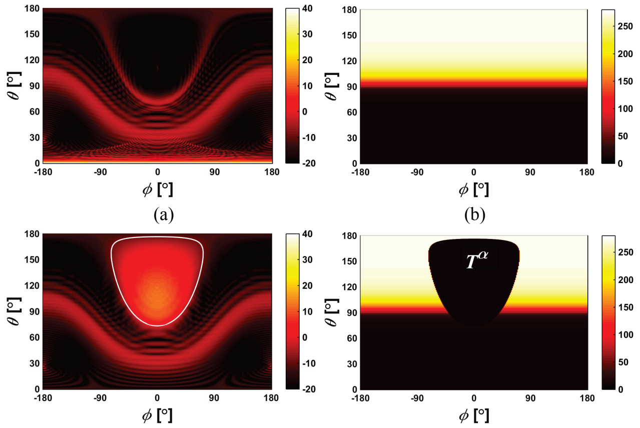

Fig. 1. For an offset Gregorian reflector system a typical antenna pattern (a) and the scene brightness temperature (b) (θ_p = 0°) as multiplied in (1) are shown. For the masking technique the pattern with the main reflector removed (c) is multiplied by the masked scene brightness temperature (θ_p = 0°) (d) as in (2).

For the method described in [2] it is assumed that all the scattered energy in the masked region is reflected into the main beam and thus toward the sky, i.e. T^{α} is the sky temperature in the pointing direction of the reflector system. The masking technique has the advantage that the number of unknowns in the EM model is greatly reduced due to the exclusion of the main reflector, and significantly fewer pattern samples are required for the convergence of the integrals in (2). This method typically underestimates the noise temperature with increasing error for electrically smaller systems. This is due to the diffraction of energy behind the main reflector causing an effective increase of background noise temperature for the energy in the direction of the main reflector mask. A diffraction compensation factor, $\alpha(f,\theta_p)$ was introduced in [3], where T^{α} is then,

$$T^{\alpha}(f,\theta_p)=[1-\alpha(f,\theta_p)]T^r+\alpha(f,\theta_p)T^d. \quad (3)$$

Here T^r is the brightness temperature in the direction of the main beam and T^d is the approximate brightness temperature behind the reflector system. For the case that $\alpha = 0$ (α^0 model) the temperature model is that given in [2]. The technique in [3] approximates α by doing a single frequency full system (including main reflector) analysis at f_1 (typically chosen at the lowest frequency of interest) and assuming inverse frequency dependence, i.e.

$$\alpha'(f,\theta_p)=\alpha(f_1,\theta_p)\frac{f_1}{f}. \quad (4)$$

This α' compensation technique works reasonably well when feeds are used with stable radiation patterns over frequency, have low edge taper, and on classical, focused reflector systems. For other cases, higher order compensation factors using two (α'') [4] and three (α''') full system analyses improve the fit to α. These models are defined as follows:

$$\alpha''(f,\theta_p) = \alpha(f_1,\theta_p)\left(\frac{f_1}{f}\right)^{n_1}, \quad (5)$$

$$\alpha'''(f,\theta_p) = \alpha(f_1,\theta_p)\left(\frac{f_1}{f}\right)^{n(f)}, \quad (6)$$

where

$$n(f) = \frac{n_1-n_2}{f_2-f_3}f + \frac{f_2 n_2 - f_3 n_1}{f_2-f_3}, \quad (7)$$

$$n_1 = \log\left(\frac{\alpha(f_2,\theta_p)}{\alpha(f_1,\theta_p)}\right) \Big/ \log\left(\frac{f_1}{f_2}\right), \quad (8)$$

$$n_2 = \log\left(\frac{\alpha(f_3,\theta_p)}{\alpha(f_1,\theta_p)}\right) \Big/ \log\left(\frac{f_1}{f_3}\right). \quad (9)$$

The frequencies f_2 and f_3 would typically, due to a lack of *a priori* information about α, be chosen at the end and in the middle of the frequency band respectively.

For comparison of the α''' model to the lower order models (α^0, α', α'') frequency subdivision was used to allow for the same number of frequency point evaluations in each model. Thus for the α'' model the frequency range was subdivided into two regions with region one in the range $[f_1, f_3]$ and region 2 in the range $[f_3, f_2]$. This model is then referred to as the α''_2 model. Similarly the α'_3 model uses the three frequency evaluations. Note that this model essentially extrapolates from each frequency point as opposed to the other models that interpolate between frequency points.

As an alternative to the compensation factor models a polynomial interpolant of the residual of the antenna temperature and the approximated antenna temperature, i.e.

$$R = T_A - T_A^{mask}, \quad (10)$$

was considered. The order of the interpolant is one less than the number of frequency points used. For the examples below three frequency points were used, thus the order of the interpolant is two, and the model is referred to as the T_A''' model.

2. Results

The accuracy of the interpolation techniques were investigated on several Gregorian reflector systems for both unshaped and shaped systems, with and without sub-reflector extensions [4] and illuminated with Gaussian feeds of various edge tapers. Only some of the results are given here. Fig. 5 shows that for a shaped system with a 16 dB edge taper, that the α' model does not fit α very well and the receiving sensitivity error is above 5%. As the model order increases the accuracy increases and for α''' the error is below 0.2% over the entire plane, i.e. frequency and elevation angles. A comparison of the various interpolation models with each using the same three frequency evaluations and frequency sub-division is given in Fig. 6. Again the α''' model has the best accuracy, however, the difference between the α''' and α''_2 models is small. Also shown in Fig. 6(b) is the error when interpolating the residual (10) plotted in Fig. 7. Although this method is perhaps easier to implement, it has slightly larger error than the compensation factor techniques.

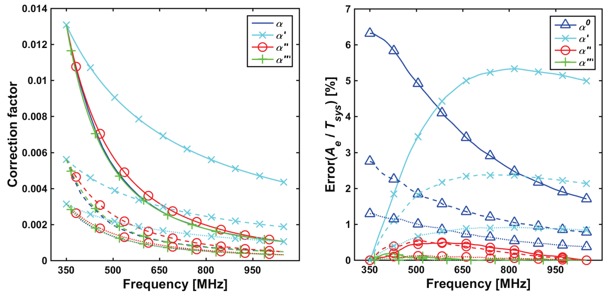

(a) (b)

Fig. 2. The (a) correction factors and (b) receiving sensitivity errors for the models without frequency sub-division on a shaped reflector system with a 20° sub-reflector extension illuminated with a Gaussian feed of edge taper 16 dB. Lines are given for $\theta_p = 0°$ (solid), $\theta_p = 35°$ (dashed), and $\theta_p = 70°$ (dotted).

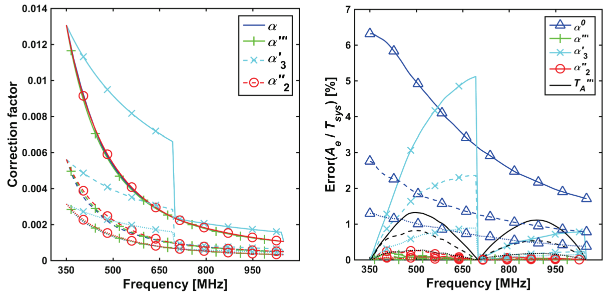

(a) (b)

Fig. 3. The (a) correction factors and (b) receiving sensitivity errors for the models using three frequencies on a shaped reflector system with a 20° sub-reflector extension illuminated with a Gaussian feed of edge taper 16 dB. Lines are given for $\theta_p = 0°$ (solid), $\theta_p = 35°$ (dashed), and $\theta_p = 70°$ (dotted).

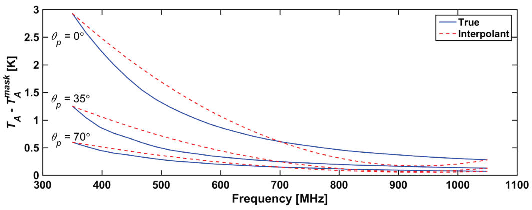

Fig. 4. A second order interpolant with three support points fitted to the residual R for the shaped reflector system with a 20° sub-reflector extension illuminated with a Gaussian feed of edge taper 16 dB.

References

[1] G. C. Medellín, "Antenna noise temperature calculation," in *SKA Memo 95*, Jul. 2007.

[2] W. A. Imbriale, "Faster antenna noise temperature calculations using a novel approximation technique," in *Proc. IEEE Int. Symp. Antennas Propag. (APSURSI)*, Toronto, ON, Canada, Jul. 2010, pp.1–4.

[3] D. I. L. de Villiers and R. Lehmensiek, "Rapid calculation of antenna noise temperature in offset Gregorian reflector systems," *IEEE Trans. Antennas Propag.*, vol. 63, no. 4, pp. 1564–1571, Apr. 2015.

[4] R. Lehmensiek and D. I. L. de Villiers, "Accuracy improvement of approximate noise temperature calculations of offset Gregorian reflector systems," in *Proc. Int. Conf. Electromagn. Adv. Appl. (ICEAA)*, Torino, Italy, Sep. 2015, pp. 847-850.

[5] R. Lehmensiek, I.P. Theron and D.I.L. de Villiers, "Deriving an optimum mapping function for the SKA shaped offset Gregorian reflectors," *IEEE Trans. Antennas Propag.*, vol. 63, no. 11, pp. 4658–4666, Nov. 2015.